Protist, Vol. 161, 91–101, January 2010
http://www.elsevier.de/protis
Published online date 7 August 2009

Protist

ORIGINAL PAPER

Purification and Characterization of a Glutathione Reductase from *Phaeodactylum tricornutum*

Diego G. Arias[a,c], Vanina E. Marquez[b], Alejandro J. Beccaria[b], Sergio A. Guerrero[a], and Alberto A. Iglesias[c,1]

[a]Laboratorio de Bioquímica Microbiana, Instituto de Agrobiotecnología del Litoral (IAL; FBCB, UNL-CONICET), Paraje "El Pozo" CC 242, Santa Fe S3000ZAA, Argentina
[b]Laboratorio de Fermentaciones, Instituto de Agrobiotecnología del Litoral (IAL; FBCB, UNL-CONICET), Paraje "El Pozo" CC 242, Santa Fe S3000ZAA, Argentina
[c]Laboratorio de Enzimología Molecular, Instituto de Agrobiotecnología del Litoral (IAL; FBCB, UNL-CONICET), Paraje "El Pozo" CC 242, Santa Fe S3000ZAA, Argentina

Submitted March 6, 2009; Accepted June 14, 2009
Monitoring Editor: Saul Purton

Glutathione reductase (E.C.1.8.1.7) was purified from *Phaeodactylum tricornutum* cells grown axenically in an autotrophic medium. The overall procedure started with preparation of the cell extract and addition of ammonium sulfate to 20% saturation, followed by anion exchange and affinity interaction chromatography (Blue-A- and 2',5'-ADP-Sepharose). Complete purification required native polyacrylamide gel electrophoresis as the final step. The enzyme was purified to homogeneity and functionally characterized. Its native molecular mass was estimated to be 118 kDa; which corresponds to a dimer. The enzyme exhibited a specific activity of 190 U mg^{-1} with an optimal activity at pH 8.0 and 32 °C. We determined K_m values of 14 μM and 60 μM for NADPH and oxidized glutathione, respectively. Products inhibited the enzyme according to a hybrid ping-pong reaction mechanism. After MALDI-TOF analysis, the purified enzyme was unambiguously identified as one of the two proteins annotated as glutathione reductases in the genome of the diatom. The properties of the enzyme help to understand redox metabolic scenarios in *P. tricornutum*.

Key words: glutathione; glutathione reductase; *Phaeodactylum tricornutum*; redox metabolism.

Introduction

Diatoms are unicellular photosynthetic algae abundant in phytoplankton, which are of particular relevance in ocean ecosystems. They are thought to be responsible for as much as 25% of global primary productivity and for an accordingly significant O_2 production (Kroth et al. 2008; Montsant et al. 2005; Oudot-Le Secq et al. 2007). These microorganisms can produce huge amounts of biomass, being estimated to be responsible for about 20% of global carbon fixation. As much as 16 gigatons of the organic carbon produced by marine phytoplankton per year, or about one third of the total oceanic production is thought to sink into the ocean interior preventing re-entrance of this carbon into the atmosphere for centuries (Kroth et al. 2008). Because most of the diatoms are surrounded by a highly structured silica cell wall, they also play a key role in the biogeochemical cycling of silicon (Montsant et al. 2005). These

[1]Corresponding author; fax +54 342 457 5209 ext. 217.
e-mail iglesias@fbcb.unl.edu.ar (A.A. Iglesias).

doi:10.1016/j.protis.2009.06.001

organisms are also used commercially for various purposes such as feeds in aquaculture, as a source of polyunsaturated fatty acids, as well as in the pharmaceutical industry (Domergue et al. 2002, 2003).

Phaeodactylum tricornutum is one of the most widely utilized model systems for studying the ecology, physiology, biochemistry and molecular biology of diatoms (Apt et al. 1996). This organism became even more attractive after the successful development of a procedure for its stable genetic transformation, which enabled the demonstration of its sensing system and its conversion into a heterotrophic organism, opening the possibility for growing it in large-scale fermentation for commercial exploitation (Apt et al. 1996; Kroth et al. 2008). Despite the relevance of *P. tricornutum*, the characterization of this alga (as it occurs for diatoms in general) with respect to its biochemistry and physiology is far from complete. A great advance to the understanding of its metabolism has been recently made with the elucidation of the entire genome (Bowler et al. 2008). After the latter, work on the purification and characterization of enzymes from the diatom is mandatory for appropriately addressing the occurrence and functionality of metabolic scenarios in *P. tricornutum*.

Glutathione reductase (glutathione:$NADP^+$ oxidoreductase, E.C.1.8.1.7; GRase), a member of the pyridine-nucleotide disulfide oxidoreductase family of flavoenzymes, catalyzes the conversion of glutathione disulfide (GSSG) to its reduced form (GSH) in the presence of NADPH (Carlberg and Mannervik 1985; Dringen and Gutterer 2002). The enzyme plays a crucial role to maintain a high intracellular [GSH]/[GSSG] ratio. GSH is a thiol-containing tripeptide widely distributed in all living organisms, where it has been shown to be involved in the regulation of protein synthesis and enzyme organization; as well as in the synthesis of the deoxyribonucleotide precursors of DNA, in the maintenance of sulfhydryl groups of proteins and in protecting cells against free radicals and other reactive oxygen species (ROS, such as H_2O_2, $O_2^{\bullet -}$ and $^{\bullet}OH$) (Carlberg and Mannervik 1985; Ulusu et al. 2005). In addition, there is an active detoxification mechanism in plants, algae and fungi that avoid heavy metal poisoning, which involves intracellular sequestration of metal ions by GSH and GSH-related peptides [(γ-Glu–Cys)*n*-Gly peptides], named phytochelatins (PCs) (Morelli and Scarano 2004; Szabo et al. 2008). These compounds are enzymatically synthesized by a PC-synthase, which uses reduced glutathione as a substrate and is activated by metal ions (as Cd^{2+}, Pb^{2+}, Zn^{2+} and Cu^{2+}) (Morelli and Scarano 2004).

In this work we report on the occurrence of GRase in *P. tricornutum*. We purified the enzyme from the unicellular microorganism and characterized it with respect to structure and kinetic properties. To the best of our knowledge, this is the first time that this enzyme is reported and studied in diatoms, these data being of relevance as groundwork for the elucidation and understanding of the physiology and metabolism of *P. tricornutum*.

Results

Isolation of GRase from *P. tricornutum*

GRase was purified from 36 g of *P. tricornutum* cells by a 5-step procedure, as summarized in Table 1. Disruption of the diatom cells by sonication rendered an extract with a high content of pigments, which interfered with the determination of enzyme activity and protein concentration. Thus, it was necessary to eliminate pigments by precipitation after the addition of ammonium sulfate to 20% saturation to have a measurable crude extract. Followed by chromatographic steps of DEAE-Sepharose, Blue-A Sepharose, and 2',5'-ADP-Sepharose, GRase was purified over 150-fold with a 16% recovery of the initial enzyme activity (Table 1). This purification protocol was found to be the more suitable for purification, after analyzing omission of some steps or changes in the order at which the different chromatographic procedures were carried out.

The sample obtained after chromatography on 2',5'-ADP-Sepharose was analyzed for purity utilizing polyacrylamide gel electrophoresis (PAGE), as illustrated in Figure 1. The sample revealed to be composed of two major proteins by native-PAGE (Fig. 1A, lane 1); and was resolved into two polypeptide bands of apparent molecular masses of 58 and 40 kDa in SDS-PAGE (Fig. 1B, lane 1). To assign GRase identity to one of the polypeptides observed in native-PAGE, the gel was stained for GRase activity with GSSG and DTNB, according to procedures previously described (Montrichard et al. 1999). After identifying the protein band that stained yellow, this band was electroeluted from a preparative native-PAGE and then concentrated by ultrafiltration. The enzyme thus obtained reached

Table 1. Purification of GRase from 36 g of *P. tricornutum* cells. Enzyme activity was assayed at 30 °C and pH 7.5.

Step	Volume (ml)	Activity (U ml^{-1})	Protein (mg ml^{-1})	Specific Activity (U mg^{-1})	Purification (fold)	Recovery (%)
Soluble extract	70	0.78	1.71	0.46	1	100
DEAE-Sepharose	18	2.12	2.59	0.82	1.8	71
Blue-A-Sepharose	4.5	5.10	0.35	14.56	32	42
2′,5′ADP-Sepharose	2.5	3.37	0.046	73.30	161	16
Native-PAGE	2.5	3.28	0.021	146.6	318	16

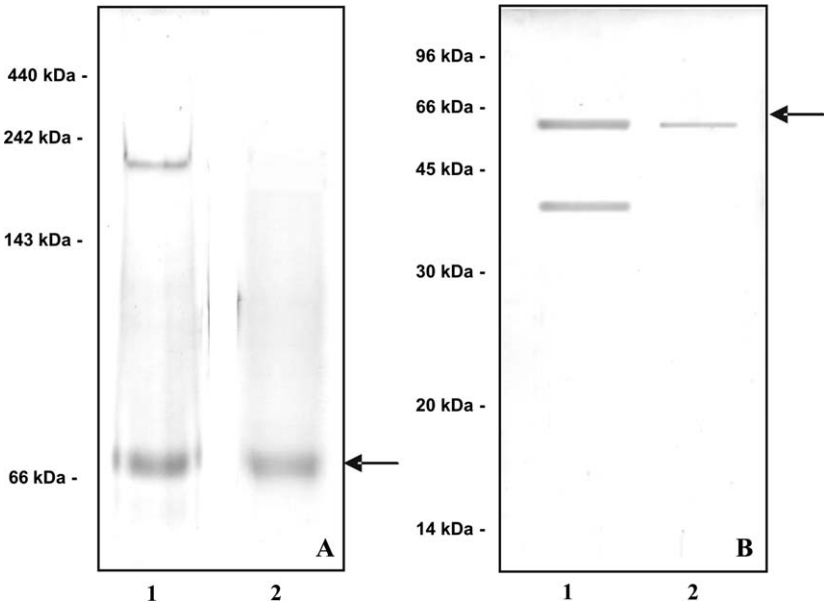

Figure 1. Electrophoretic analysis of purified *Pt*GRase-1. Proteins were separated using: (**A**) 6% (w/v) native PAGE or (**B**) 15% (w/v) SDS–PAGE, followed by staining of the gels with Coomassie blue. Lane 1: protein eluted from 2′,5′-ADP Sepharose. Lane 2: electroeluted protein with GRase activity.

a specific activity of 142 U mg^{-1} at pH 7.5 (Table 1) and 196 U mg^{-1} at pH 8.0, and it migrated as a single protein band in native-PAGE (Fig. 1A, lane 2).

Structural and Kinetic Characterization

The amino acid sequence of the pure enzyme, determined by MALDI-TOF, completely matched with one (NCBI Accession No. XP_002180322) of the two sequences annotated as GRases in the genome project of *P. tricornutum* (Bowler et al. 2008). The primary structure of this purified enzyme (that we now call *Pt*GRase-1) indicates that it consists of 496 amino acids with a calculated pI of 5.03 and 53,470 Da molecular mass. The calculated size of the protein is in good agreement with the molecular mass of about 58 kDa determined for the single polypeptide in SDS-PAGE of purified *Pt*GRase-1 (Fig. 1B, lane 2). The migration profile of the purified enzyme in SDS-PAGE was not dependent on the presence or absence of DTT in the running buffer. On the other hand, the purified *Pt*GRase-1 migrated as a protein of 118 kDa in native-PAGE (Fig. 2), thus revealing that the enzyme forms a homodimeric structure in its native, active state.

Purified *Pt*GRase-1 exhibited an absorption spectrum with a pattern typical of a flavin-containing protein (Fig. 3), characterized by two peaks of maximal absorption at 358 and 452 nm. As shown in Figure 3, after reduction of the

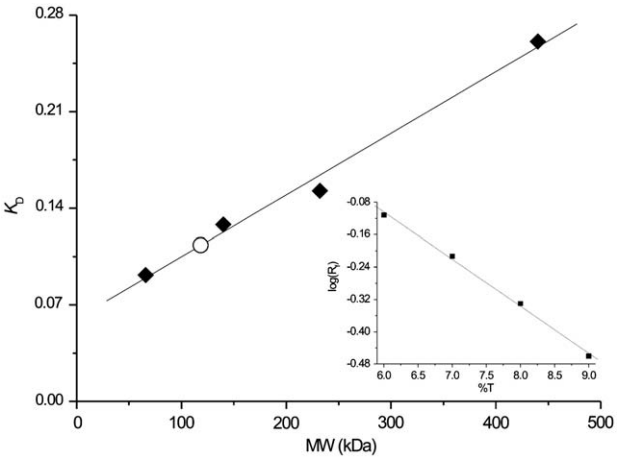

Figure 2. Determination of native molecular weight of *Pt*GRase-1. Secondary Ferguson plot (Ferguson 1964) was generated by plotting retardation coefficients (K_D) vs. molecular mass for protein standards (◆): ferritin (440 kDa); catalase (232 kDa); lactate dehydrogenase (140 kDa) and albumin (66 kDa). Retardation coefficient for the purified *Pt*GRase-1 (○) was calculated to be 0.111, which correlates with an estimated molecular mass of 118 kDa. Inset: Primary Ferguson plot was generated by plotting log of electrophoretic mobility (log R_f) of purified *Pt*GRase-1 vs. gel concentration (%T).

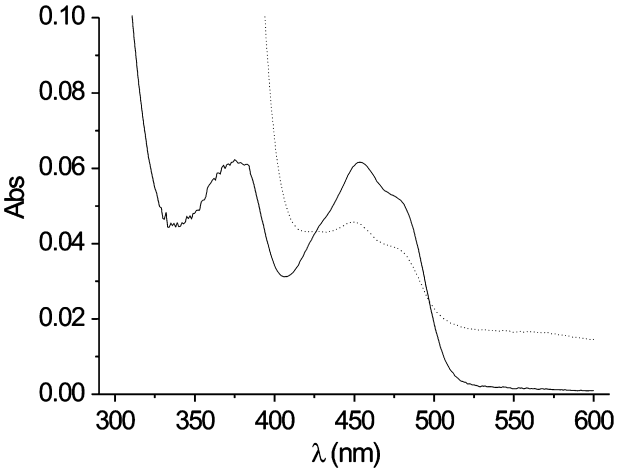

Figure 3. Absorption spectrum of purified *Pt*GRase-1 (0.18 mg ml^{-1} or 3.1 μM), performed in 20 mM TRIS-HCl pH 8.0; 1 mM EDTA, at 25 °C. In solid line: the purified *Pt*GRase-1 without additives and in dot lines the purified *Pt*GRase-1 in the presence of 200 μM NADPH.

enzyme with an excess of NADPH, the absorbance at 452 nm decreases concomitantly with an absorption increase around 550-560 nm. This has been attributed to the optical consequence of a charge transfer in the GRase···NADPH complex between a thiolate anion and the isoalloxazine ring, which is amplified by the presence of NADPH (Pai and Schulz 1983; Serrano et al. 1984).

Figure 4 shows the amino acid sequence alignments between *Pt*GRase-1 and the enzyme from different organisms. In the alignment we included the sequence predicted from the other gene reported in *P. tricornutum* as putatively coding for GRase (Bowler et al. 2008). The latter enzyme (that we call here *Pt*GRase-2; NCBI Accession No. XP_002183930 corresponds to a protein of 507 amino acids that shares 54.8% identity and 65.1% similarity with *Pt*GRase-1 (see Fig. 4 for a comparison). Structurally, the enzyme from the diatom seems more related to the protein from bacteria, protozoa, and mammals (sharing identities and similarities of about 45% and 55%, respectively), than with the enzyme from green algae or land plants (sharing identities and similarities of about 35% and 50%, respectively) (see Fig. 4 for details).

*Pt*GRase-1 catalyzed reduction of GSSG and GSNO utilizing NADPH but not NADH as electron donor (Fig. 5). The enzyme was not effective to reduce cystine, lipoamide, nor trypanothione disulphide (Fig. 5). Also shown in Figure 5 is that DTNB reductase activity was detected in the presence of glutathione as a mediator. Using levels up to 300 μM $NADP^+$ and 1 mM GSH, the enzyme did not catalyze the reverse reaction, indicating that its physiological function is the reduction of GSSG or GSNO but not the opposite. Hyperbolic saturation kinetics for all the substrates, NADPH (data not shown), GSSG and GSNO were observed (Fig. 6). The double reciprocal plots of initial velocity versus GSSG concentration, determined at four different concentrations of NADPH showed parallel lines, which supports a ping-pong mechanism for *Pt*GRase-1 (Fig. 7). The kinetic parameters for NADPH, GSSG and GSNO are shown in Table 2. The enzyme exhibited higher affinity for GSSG than for GSNO, but k_{cat} values for reduction of either of the substrates were quite similar. Results indicate that the difference in catalytic efficiency (k_{cat} Km^{-1}) for theses substrates is mainly a consequence of changes in the binding step rather than in the actual catalytic process.

The latter was found to be reinforced by studying inhibitory effects caused by the products, $NADP^+$ and GSH, with results being summarized in Table 3. Under non-saturating conditions for NADPH (<50 μM) or GSSG

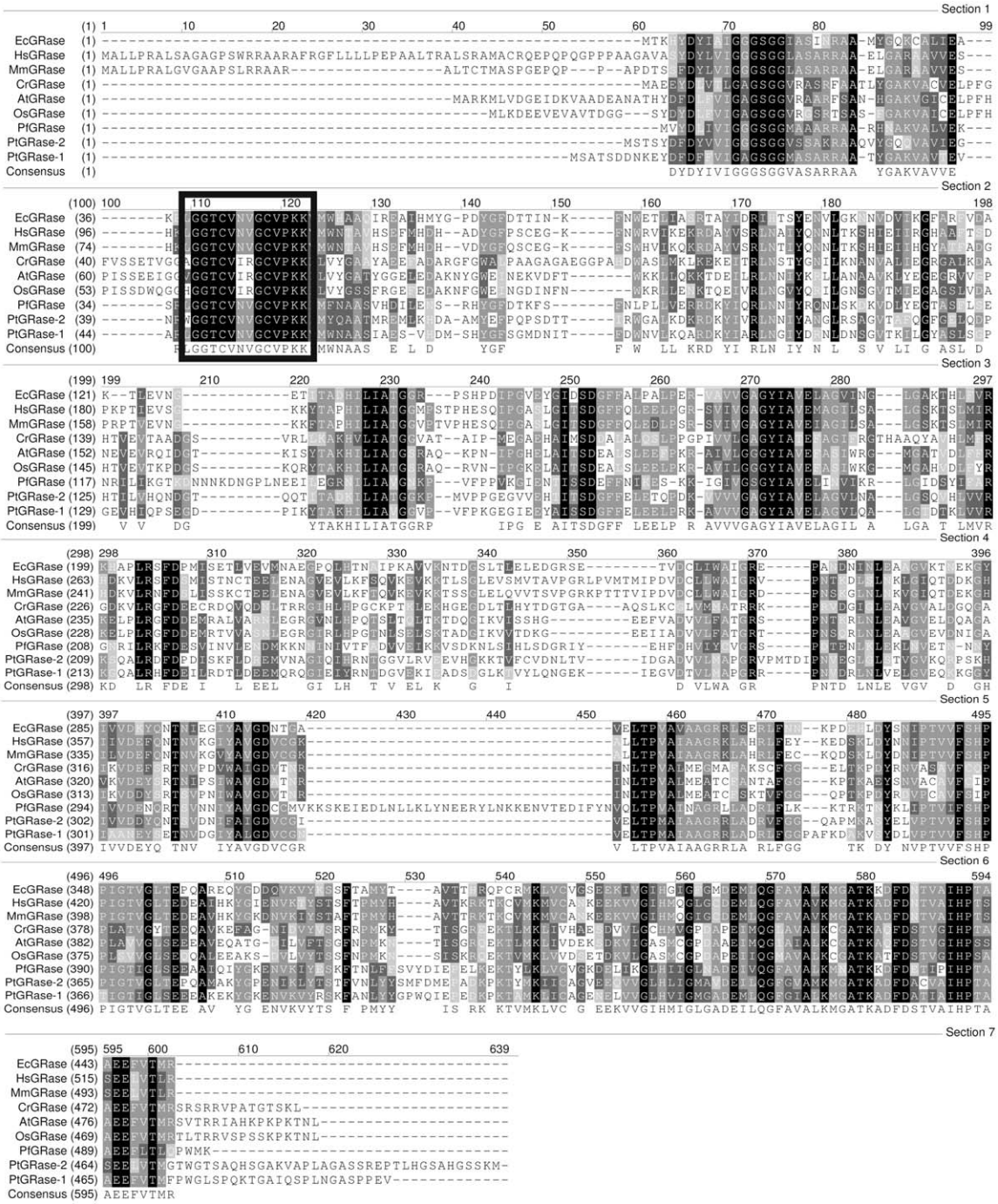

Figure 4. Sequence alignment of *Pt*GRase-1 with *Pt*GRase-2 and homologue enzymes from *Escherichia coli* (NCBI Accession No. NP_312399), *Homo sapiens* (NCBI Accession No. NP_000628), *Mus musculus* (NCBI Accession No. CAA53959), *Chlamydomonas reinhardtii* (NCBI Accession No. XP_001696579), *Arabidopsis thaliana* (NCBI Accession No. AAB67841), *Oryza sativa* (NCBI Accession No. BAA36283) and *Plasmodium falciparum* (NCBI Accession No. AAB84117). Each individual sequence is numbered accordingly. The black box indicates the redox active motif (CXXXXC).

(<200 μM), $NADP^+$ was inhibitory. However, $NADP^+$ (up to 1 mM) was not inhibitor when assays were performed at 1 mM GSSG and 300 μM NADPH. GSH functioned as an inhibitor at relatively high concentrations (>1 mM), and also only in the lower substrate concentration

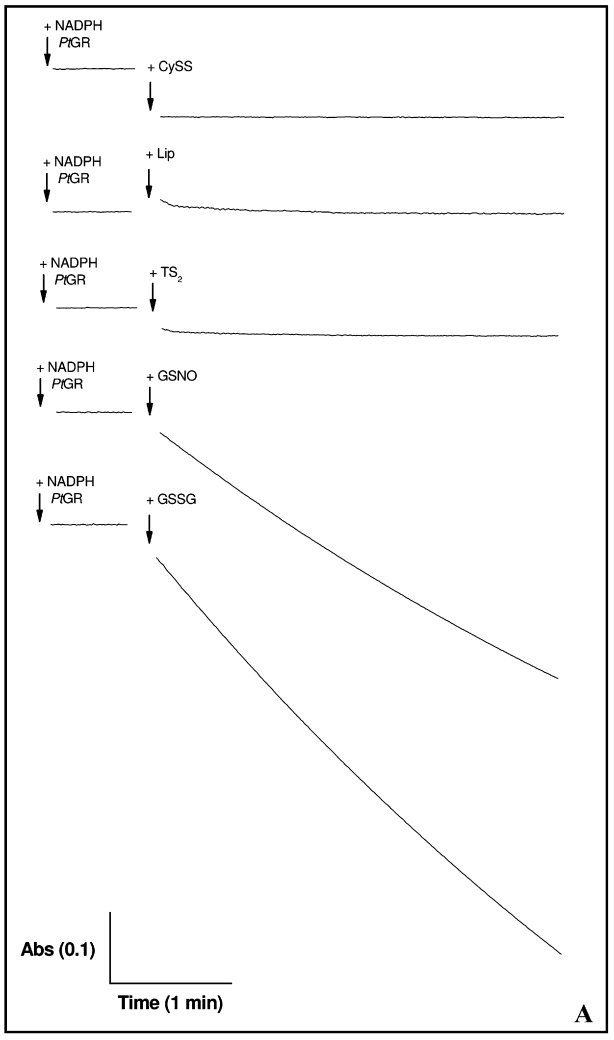

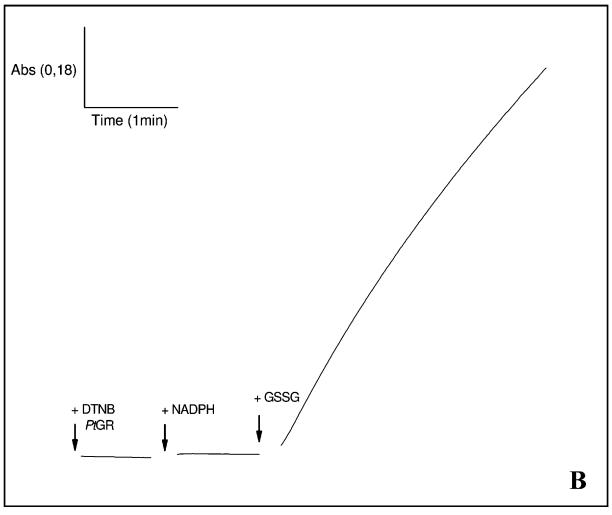

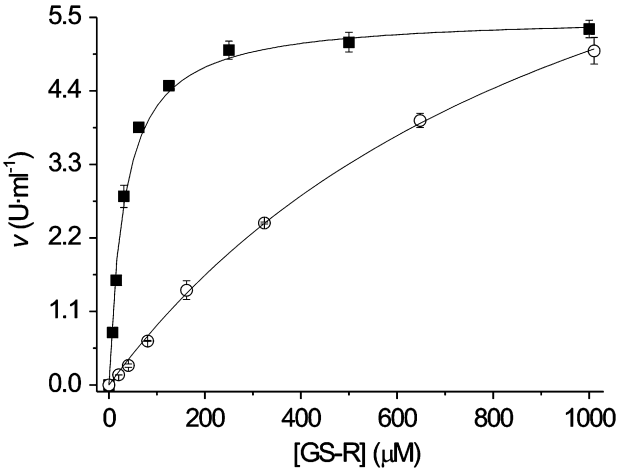

Figure 6. Saturation curves for the reduction of GSSG and GSNO by *Pt*GRase-1. The reactions were performed in 100 mM TRIS-HCl pH 8.0, 2 mM EDTA, 300 μM NADPH, 2.4 nM *Pt*GRase-1 and different concentrations of (■) GSSG or (○) GSNO, at 30 °C.

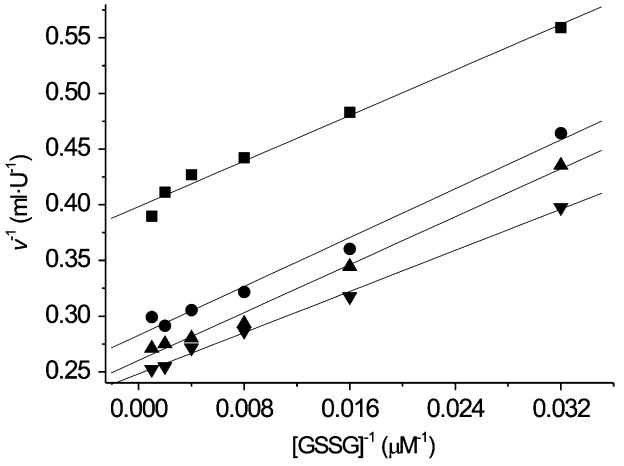

Figure 7. Kinetic analysis of *Pt*GRase-1. Reactions were performed in 100 mM TRIS-HCl pH 8.0, 2 mM EDTA, 2.4 nM *Pt*GRase-1, 0-1 mM GSSG and different concentrations of NADPH: (■) 8.6 μM; (●) 17 μM; (▲) 26 μM and (▼) 34 μM, at 30 °C.

Figure 5. Assay of the NADPH-dependent reductase activity of *Pt*GRase-1. The reaction mixture contained 100 mM TRIS-HCl pH 8.0; 2 mM EDTA; 200 μM NADPH and 1 mM CysS or 1 mM Lip or 0.25 mM TS_2 or 1 mM GSNO or 1 mM GSSG (**A**) or 1 mM DTNB (**B**), respectively.

Table 2. Kinetic parameters for the substrates of *Pt*GRase-1 determined at pH 8.0 and 30 °C.

Substrate	k_{cat} (s^{-1})	*K*m (μM)	$k_{cat} \cdot Km^{-1}$ ($M^{-1} s^{-1}$)
NADPH	190	14	$1.36 \cdot 10^7$
GSSG	190	60	$3.17 \cdot 10^6$
GSNO	181	818	$2.21 \cdot 10^5$

Table 3. Product inhibition constants of *Pt*GRase-1 determined at pH 8.0 and 30 °C.

Inhibitor	Type of inhibition	K_i
$NADP^+$	Competitive regarding NADPH	52 μM
$NADP^+$	Non-competitive with regard to GSSG	1 mM
GSH	Non-competitive regarding NADPH	10 mM
GSH	Competitive with regard to GSSG	5 mM

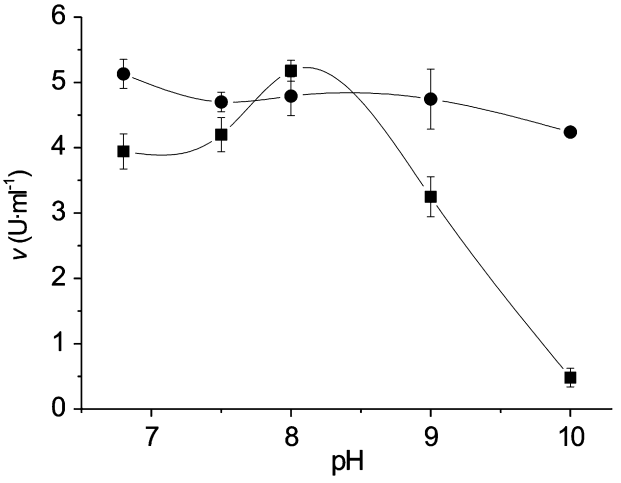

Figure 8. Effect of pH on the activity (■) and stability (●) of *Pt*GRase-1. Reactions were performed in 100 mM TRIS-HCl; 2 mM EDTA; 300 μM NADPH, 1 mM GSSG and 2.4 nM *Pt*GRase-1, at 30 °C.

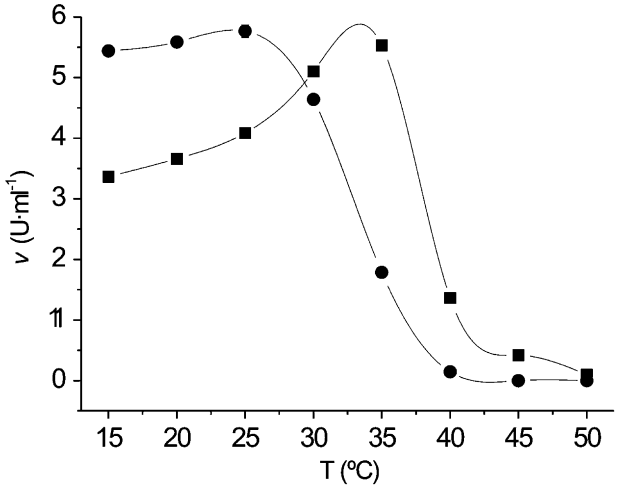

Figure 9. Effect of temperature on the activity (■) and stability (●) of *Pt*GRase-1. Reactions were performed in 100 mM TRIS-HCl pH 8.0; 2 mM EDTA; 300 μM NADPH, 1 mM GSSG and 2.4 nM *Pt*GRase-1.

range. A kinetic analysis showed that inhibition by GSH was non-competitive with respect to NADPH and competitive with respect to GSSG; whereas $NADP^+$ behaved as a non-competitive or competitive inhibitor respect to GSSG or NADPH, respectively. An integrated analysis of the types of inhibition by products with respect to substrates supports a hybrid ping-pong mechanism for the reaction (Cenas et al. 2004; Huber and Brandt 1980; Pai and Schulz 1983; Serrano et al. 1984).

Activity (assayed as reduction of GSSG with NADPH) of *Pt*GRase-1 was optimal at pH 8.0, in 100 mM TRIS-HCl buffer, in which the enzyme was stable in the range of pH 6.5-10 (Fig. 8). The activity remained practically unchanged between pH 6.5-7.5 and it decreased significantly only above pH 8.5 (Fig. 8). Concerning the behavior of *Pt*GRase-1 in relation to temperature, Figure 9 shows that optimal enzyme activity was reached at 35 °C. The abrupt decrease in activity observed at temperatures higher than 35 °C, could be associated with loss of enzyme stability beyond 30 °C (Fig. 9), The apparent activation energy of the reaction was calculated (using data from Figure 9, over the range of 15-35 °C) to be 22,358 J mol^{-1}. On the other hand, *Pt*GRase-1 activity was very sensitive to inhibition by Cu^{2+} (IC_{50}=3.4 μM) and Zn^{2+} (IC_{50}=4.2 μM), with Co^{2+} exhibiting a more moderate effect (IC_{50}= 36 μM),

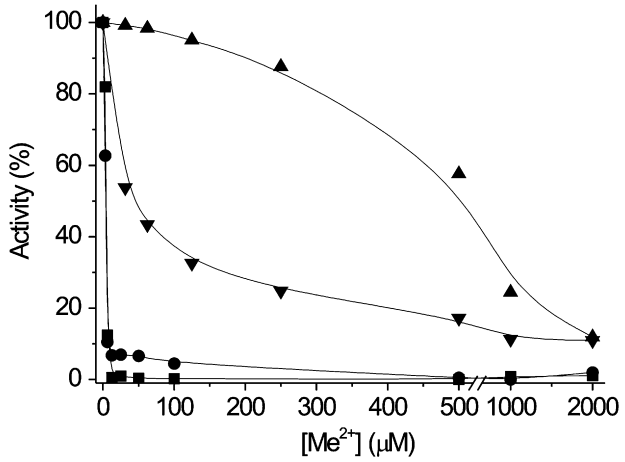

Figure 10. Inhibition of *Pt*GRase-1 by heavy metal ions. Enzyme assays were performed in 100 mM TRIS-HCl pH 8.0; 300 μM NADPH, 1 mM GSSG, 2.4 nM *Pt*GRase-1 and different concentration of metals: (■) Zn^{2+}; (●) Cu^{2+}; (▲) Ni^{2+} and (▼) Co^{2+}, at 30 °C.

whereas Ni^{2+} inhibited activity with an IC_{50} of 534 μM (Fig. 10).

Discussion

In the present study we have isolated and characterized *Pt*GRase-1, thus named after establishing identity with the coding product of one of the two genes annotated in the genome of *P. tricornutum* as coding for GRases (Bowler et al. 2008). To the best of our knowledge, this is the first detailed study about this type of enzyme from a diatom. The purification procedure described here was efficient to obtain a pure enzyme, on the basis of electrophoretic criteria, and with a specific activity of 196 U mg^{-1} at 30 °C and pH 8.0. This activity value is very close to others reported for GRases purified from different sources (Carlberg and Mannervik 1975, 1985; Chung and Hurlbert 1975; Dringen and Gutterer 2002; Serrano et al. 1984). The enzyme has been extensively studied in animals (Dringen and Gutterer 2002; Erat et al. 2003, 2005; Garcia-Alfonso et al. 1993; Ulusu et al. 2005), yeast (Colman and Black 1965; Huber and Brandt 1980; Massey and Williams 1965; Rakauskiene et al. 1989), land plants (Anderson et al. 1990; Connell and Mullet 1986; Madamanchi et al. 1992) and cyanobacteria (Serrano et al. 1984); but scarcely studied in diatoms or other algae (in *Euglena gracilis* strain Z, GRase has been previously studied by Montrichard et al. 1999 and Shigeoka et al. 1987).

*Pt*GRase-1 was characterized as a homodimer of 118 kDa, which is in accordance with the size and structure of many GRases (Carlberg and Mannervik 1985; Dringen and Gutterer 2002; Shigeoka et al. 1987), except the enzyme from the photosynthetic bacterium *Rhodospirillum rubrum* and some others from mammalian tissues (such as brain), which are monomeric proteins (Dringen and Gutterer 2002; Serrano et al. 1984). The enzyme purified from the diatom, exhibited spectral properties typical of a flavin-containing protein. Additionally, the absorption spectrum of the enzyme exhibited changes upon incubation with an excess of NADPH, which has been ascribed to the formation of an electron paramagnetic resonance-silent charge-transfer complex for other GRases when reduced by the pyridine nucleotide (Carlberg and Mannervik 1975; Scott et al. 1963; Serrano et al. 1984).

Using double-reciprocal plots of GSSG concentration versus reaction velocity, the enzyme systems gave parallel lines, suggesting that the mechanism of *Pt*GRase-1 is a binary complex or two-site ping-pong mechanism; these facts are consistent with GRase characterized from different sources (Erat et al. 2003; Garcia-Alfonso et al. 1993; Shigeoka et al. 1987). In addition, the kinetic data suggest a hybrid ping-pong mechanism that support the occurrence of two binding sites for each substrate in the enzyme that can be in a reduced or oxidized state (Bironaite et al. 1998; Cenas et al. 2004; Pai and Schulz 1983). The k_{cat} and K_m values for GSSG and NADPH were consistent with the values found for other GRases, as well as the optimum pH and temperature (8.0 and 32 °C respectively) (Carlberg and Mannervik 1985; Dringen and Gutterer 2002; Rakauskiene et al. 1989; Shigeoka et al. 1987). Like the enzyme from photosynthetic organisms, including purple bacteria and *E. gracilis* (Madamanchi et al. 1992; Serrano et al. 1984; Shigeoka et al. 1987), the purified *Pt*GRase-1 exhibited a strong preference for NADPH (the main reduced product of the photosynthetic electron transport chain). These catalytic properties of the enzyme could suggest an adaptation to the cellular environment in which it works.

Alternatively, *Pt*GRase-1 presented the capacity to reduce GSNO. Although the catalytic efficiency for GSNO reduction is one order of magnitude lower than for GSSG reduction, the former is higher with respect to other members of the pyridine nucleotide disulfide oxidoreductase family, such as thioredoxin

reductase from mammals (Nikitovic and Holmgren 1996) or protozoa [e.g., the enzyme from *Plasmodium falciparum* (Kanzok et al. 2000)]. These results are worth mentioning, considering that GRases from other sources, such as humans (Becker et al. 1995), yeast (Nikitovic and Holmgren 1996) and rat liver (Nikitovic and Holmgren 1996) do not exhibit the capacity to reduce GSNO, or even are inhibited irreversibility by this compound. The latter suggests that *Pt*GRase-1 (and possibly other proteins involved in GSH metabolism in the diatom, such as glutaredoxin) may participate in mechanisms regulating intracellular concentrations of GSNO, which would be a potential endogenous oxidant from the own photosynthetic aerobic metabolism of the diatom.

We have found that *Pt*GRase-1 is strongly inhibited by heavy metal ions (principally Cu^{2+} and Zn^{2+}), which could act through the irreversible binding of the cation thiol groups of the enzyme. On the other hand, we observed that both $NADP^+$ and GSH (the reaction products) inhibit the enzyme with high K_i values. This phenomena could be due to the high standard reduction potential of GSH (-0.24 V) with respect to NADPH (-0.32 V), that better supports the reaction of GSSG reduction (Scott et al. 1963; Shigeoka et al. 1987). Glutathione, the most important intracellular thiol in *P. tricornutum* (Morelli and Scarano 2004), plays a key role in the protection against reactive oxygen species generated during photosynthesis, and also in the maintenance of the intracellular redox equilibrium. Alternatively, GSH and derived peptides such as PC, form the first line of defense against heavy metal-mediated free radical formation (Morelli and Scarano 2004). Consequently, GRase, an enzyme responsible for preserving this compound in its reduced state, turns into a key component of the algal redox scenario.

Our results strongly support the occurrence of the GSH system in *P. tricornutum*, which represents valuable information for the incipient diatom proteome. Although more work is necessary to elucidate the redox metabolism in this microorganism, it seems clear that these eukaryotes comprise a simple and appropriate system to study the relationships between glutathione metabolism and evolution of photosynthesis.

Methods

Chemicals, organism and culture: NADPH, GSSG, cystine, lipoamide, and 2',5'-ADP-Agarose were purchased from Sigma (St. Louis, MO, USA). DEAE-Sepharose, and Blue-A-Sepharose were from GE Healthcare Life Sciences. All other chemicals were of the highest quality commercially available.

P. tricornutum [strain LFF Pt 01 from Laboratorio de Fermentaciones, FBCB, UNL (strain available upon request, e-mail: abeccari@)fbcb.unl.edu.ar)] cells were grown under illumination (92 $\mu E\,m^{-2}\,s^{-1}$) in artificial seawater culture medium (Berges et al. 2001) at 22 °C with aeration. After 4 days, the cells were harvested by centrifugation (500 × g, 15 min) and stored at –20 °C.

Purification of GRase: All purification steps were carried out at 4 °C. The *P. tricornutum* cell pellet (36 g) was resuspended in buffer A (20 mM TRIS-HCl, pH 8.0, containing 1 mM EDTA). The cell suspension was disrupted by sonication and centrifuged during 40 min at 9000 × g. To the resulting soluble fraction, powdered ammonium sulfate was slowly added to reach 30% saturation of the salt. After dialysis against buffer A, the sample was applied on a DEAE-Sepharose column (10 ml) previously equilibrated with buffer A. After washing with 10-bed volumes of buffer A, the enzyme was eluted by applying a gradient of 0 to 1 M NaCl in the same buffer. Fractions containing GRase activity were pooled, dialyzed against buffer A, and loaded onto a 5 ml Blue-A Sepharose column. Washing and enzyme eluting conditions for this column was performed as for the previous step. The resulting sample was dialyzed against buffer A and onto a 2′5′-ADP Agarose column (2 ml), also processed as before. Fractions containing GRase activity were pooled, concentrated by ultrafiltration and resolved in an 6% preparative native-PAGE (in 360 mM TRIS-HCl, pH 8.8 at 4 °C), conducted in 25 mM TRIS, 192 mM glycine, pH 8.8 at 30 mA. The gel was stained for GRase activity as previously described (Montrichard et al. 1999). The enzyme was recovered from the band exhibiting activity by electroelution using the Model 422 Electro-Eluter apparatus (BIO-RAD) at 4 °C, during 4 h at 10 mA, in buffer TRIS-glycine pH 8.8. The electroeluted protein was then concentrated by ultrafiltration.

Enzyme assay and kinetics: All enzyme assays were performed in a Multiskan scent one-channel vertical light path filter photometer (Thermo Electron Co), at 30 °C, and a final volume of 250 µl. One unit (U) of activity is defined as the amount of enzyme catalyzing the oxidation of 1 µmol NADPH per minute under the conditions specified in each case.

GRase activity was assayed according to previous protocols (Dringen and Gutterer 2002; Shigeoka et al. 1987) in a reaction mixture containing 100 mM TRIS-HCl (pH 8.0), 2 mM EDTA, 0.3 mM NADPH, 1 mM GSSG, and one adequate amount of enzyme. The reaction was initiated by the addition of GSSG and followed by measuring decrease in absorbance at 340 nm. Analysis of activities of GSNO reductase, cystine reductase (Scott et al. 1963), dihydrolipoamide dehydrogenase (Scott et al. 1963), and trypanothione reductase (Krauth-Siegel et al. 1987; Montrichard et al. 1999) were performed under identical conditions, except that GSSG was omitted and replaced by 1 mM GSNO, 1 mM cystine, 1 mM lipoamide, or 0.25 mM trypanothione disulphide, respectively. DTNB reductase activity was assayed in the same reaction mixture with the addition of 1 mM DTNB instead of GSSG, but the reaction was monitored following the increase in absorbance at 405 nm (Montrichard et al. 1999).

The kinetic parameters were acquired by fitting the data with a nonlinear least-square formula and the Michaelis-Menten equation. Kinetic constants are the mean of at least three independent sets of data, and they are reproducible within ± 10%. In the study of inhibitors, IC_{50} refers to the concentration of the inhibitor giving 50% of the initial activity.

Effect of pH and temperature on protein stability and activity: To evaluate protein stability, the purified *Pt*GRase was incubated at 30 °C for 5 min at pH values ranging from 7.0 to 10.0. Alternatively, the purified enzyme was incubated at pH 8.0 for 5 min at temperatures ranging from 15 to 60 °C. In both

assays, an aliquot of the mixture was taken after the treatment and assayed for activity (in the NADPH-dependent GSSG reduction direction) under the above described standard conditions of pH and temperature.

The effect of pH and temperature was further evaluated by measuring activity at different values of each of the variables. Thus, *Pt*GRase activity was measured at pH values ranging from 7.0 to 10.0 in 100 mM TRIS-HCl at 30 °C, or at temperature values ranging from 15 to 60 °C in 100 mM TRIS-HCl pH 8.0.

Protein methods: Native–PAGE and SDS-PAGE were carry out using the Bio-Rad minigel equipment, basically according to previously described methods (Laemmli 1970). Coomassie brilliant blue was used to stain protein bands. Determination of native molecular mass was carry out by native-PAGE with varying crosslinking degrees of polyacrylamide, according to Ferguson′s method, using 6, 7, 8 and 9% native gels (Ferguson 1964). Protein contents were determined by the method of Bradford (Bradford 1976), utilizing BSA as a standard.

Preparation of GSNO: GSNO was prepared as previously described (Gordge et al. 1998) by nitrosation under acid conditions. Briefly, equal volumes of glutathione (100 mM) and sodium nitrite (100 mM) were incubated in the presence of 10 mM HCl on ice for 30 min. GSNO was stabilized by the addition of 1 mM EDTA. GSNO was freshly prepared each day and stored on ice in the dark until used. The concentration of GSNO was estimated by its absorbance at 334 nm using a molar absorption coefficient of 0.85 $mM^{-1}\,cm^{-1}$.

MALDI-TOF: The amino acid sequence of the purified GRase was analyzed by matrix-assisted laser desorption and ionization time-of flight (MALDI-TOF) mass spectrometry in the Unit of Analytical Biochemistry and Proteomics at the Institut Pasteur (Montevideo, Uruguay). Briefly, the samples were faded, washed and resuspended in 30 mM NH_4HCO_3, pH 8.0; and incubated with trypsin (sequencing grade, Promega). The peptides were extracted with 60% acetonitrile, 0.1% trifluoroacetic acid. Then, the samples were concentrated by a Speed-Vac and finally desalted with a reverse phase micro-column. The elution was directly loaded on the equipment plate with a matrix solution (α-cyano-4-hydroxy-cinnamic acid in 60% acetonitrile and 0.2% trifluoroacetic acid) (Parodi-Talice et al. 2004, 2007). Peptide profiles were analyzed with a Mascot server (www.matrixscience.com).

Acknowledgements

This work was supported by grants from ANPCyT (PICT′03 1-14733; PAV′03 137, PICTO′05 13129), CONICET (PIP 6358), UNL (CAI+D 2006). VEM is a fellow and AJB an investigator from UNL. DGA is a fellow from CONICET, and SAG and AAI are investigator career members from the same institution.

References

Anderson JV, Hess JL, Chevone BI (1990) Purification, characterization, and immunological properties for two isoforms of glutathione reductase from eastern white pine needles. Plant Physiol **94**:1402–1409

Apt KE, Kroth-Pancic PG, Grossman AR (1996) Stable nuclear transformation of the diatom *Phaeodactylum tricornutum*. Mol Gen Genet **252**:572–579

Becker K, Gui M, Schirmer RH (1995) Inhibition of human glutathione reductase by S-nitrosoglutathione. Eur J Biochem **234**:472–478

Berges JA, Franklin DJ, Harrison PJ (2001) Evolution of an artificial seawater medium: improvements in enriched seawater, artificial water over the last two decades. J Phycol **37**:1138–1145

Bironaite D, Anusevicius Z, Jacquot JP, Cenas N (1998) Interaction of quinones with *Arabidopsis thaliana* thioredoxin reductase. Biochim Biophys Acta **1383**:82–92

Bowler C, Allen AE, Badger JH, Grimwood J, Jabbari K, Kuo A, Maheswari U, Martens C, Maumus F, Otillar RP, Rayko E et al (2008) The *Phaeodactylum* genome reveals the evolutionary history of diatom genomes. Nature **456**:239–244

Bradford MM (1976) A rapid and sensitive method for the quantitation of microgram quantities of protein utilizing the principle of protein–dye binding. Anal Biochem **72**:248–254

Carlberg I, Mannervik B (1975) Purification and characterization of the flavoenzyme glutathione reductase from rat liver. J Biol Chem **250**:5475–5480

Carlberg I, Mannervik B (1985) Glutathione reductase. Methods Enzymol **113**:484–490

Cenas N, Nivinskas H, Anusevicius Z, Sarlauskas J, Lederer F, Arner ES (2004) Interactions of quinones with thioredoxin reductase: a challenge to the antioxidant role of the mammalian selenoprotein. J Biol Chem **279**:2583–2592

Colman RF, Black S (1965) On the role of flavin adenine dinucleotide and thiol groups in the catalytic mechanism of yeast glutathione reductase. J Biol Chem **240**:1796–1803

Connell JP, Mullet JE (1986) Pea chloroplast glutathione reductase: purification and characterization. Plant Physiol **82**:351–356

Chung YC, Hurlbert RE (1975) Purification and properties of the glutathione reductase of *Chromatium vinosum*. J Bacteriol **123**:203–211

Domergue F, Lerchl J, Zahringer U, Heinz E (2002) Cloning and functional characterization of *Phaeodactylum tricornutum* front-end desaturases involved in eicosapentaenoic acid biosynthesis. Eur J Biochem **269**:4105–4113

Domergue F, Spiekermann P, Lerchl J, Beckmann C, Kilian O, Kroth PG, Boland W, Zahringer U, Heinz E (2003) New insight into *Phaeodactylum tricornutum* fatty acid metabolism. Cloning and functional characterization of plastidial and microsomal delta12-fatty acid desaturases. Plant Physiol **131**:1648–1660

Dringen R, Gutterer JM (2002) Glutathione reductase from bovine brain. Methods Enzymol **348**:281–288

Erat M, Demir H, Sakiroglu H (2005) Purification of glutathione reductase from chicken liver and investigation of kinetic properties. Appl Biochem Biotechnol **125**:127–138

Erat M, Sakiroglu H, Ciftci M (2003) Purification and characterization of glutathione reductase from bovine erythrocytes. Prep Biochem Biotechnol **33**:283–300

Ferguson KA (1964) Starch-gel electrophoresis – application to the classification of pituitary proteins and polypeptides. Metabolism **13** (Suppl)985–1002

Garcia-Alfonso C, Martinez-Galisteo E, Llobell A, Barcena JA, Lopez-Barea J (1993) Horse-liver glutathione reductase: purification and characterization. Int J Biochem **25**:61–68

Gordge MP, Hothersall JS, Noronha-Dutra AA (1998) Evidence for a cyclic GMP-independent mechanism in the anti-platelet action of S-nitrosoglutathione. Br J Pharmacol **124**:141–148

Huber PW, Brandt KG (1980) Kinetic studies of the mechanism of pyridine nucleotide dependent reduction of yeast glutathione reductase. Biochemistry **19**:4569–4575

Kanzok SM, Schirmer RH, Turbachova I, Iozef R, Becker K (2000) The thioredoxin system of the malaria parasite *Plasmodium falciparum*. Glutathione reduction revisited. J Biol Chem **275**:40180–40186

Krauth-Siegel RL, Enders B, Henderson GB, Fairlamb AH, Schirmer RH (1987) Trypanothione reductase from *Trypanosoma cruzi*. Purification and characterization of the crystalline enzyme. Eur J Biochem **164**:123–128

Kroth PG, Chiovitti A, Gruber A, Martin-Jezequel V, Mock T, Parker MS, Stanley MS, Kaplan A, Caron L, Weber T, Maheswari U et al (2008) A model for carbohydrate metabolism in the diatom *Phaeodactylum tricornutum* deduced from comparative whole genome analysis. PLoS ONE **3**:e1426

Laemmli UK (1970) Cleavage of structural proteins during the assembly of the head of bacteriophage T4. Nature **227**:680–685

Madamanchi NR, Anderson JV, Alscher RG, Cramer CL, Hess JL (1992) Purification of multiple forms of glutathione reductase from pea (*Pisum sativum* L.) seedlings and enzyme levels in ozone-fumigated pea leaves. Plant Physiol **100**:138–145

Massey V, Williams Jr CH (1965) On the reaction mechanism of yeast glutathione reductase. J Biol Chem **240**:4470–4480

Montrichard F, Le Guen F, Laval-Martin DL, Davioud-Charvet E (1999) Evidence for the co-existence of glutathione reductase and trypanothione reductase in the non-trypanosomatid Euglenozoa: *Euglena gracilis* Z. FEBS Lett **442**:29–33

Montsant A, Jabbari K, Maheswari U, Bowler C (2005) Comparative genomics of the pennate diatom *Phaeodactylum tricornutum*. Plant Physiol **137**:500–513

Morelli E, Scarano G (2004) Copper-induced changes of non-protein thiols and antioxidant enzymes in the marine microalga *Phaeodactylum tricornutum*. Plant Science **167**:289–296

Nikitovic D, Holmgren A (1996) S-nitrosoglutathione is cleaved by the thioredoxin system with liberation of glutathione and redox regulating nitric oxide. J Biol Chem **271**:19180–19185

Oudot-Le Secq MP, Grimwood J, Shapiro H, Armbrust EV, Bowler C, Green BR (2007) Chloroplast genomes of the diatoms *Phaeodactylum tricornutum* and *Thalassiosira pseudonana*: comparison with other plastid genomes of the red lineage. Mol Genet Genomics **277**:427–439

Pai EF, Schulz GE (1983) The catalytic mechanism of glutathione reductase as derived from X-ray diffraction analyses of reaction intermediates. J Biol Chem **258**:1752–1757

Parodi-Talice A, Duran R, Arrambide N, Prieto V, Pineyro MD, Pritsch O, Cayota A, Cervenansky C, Robello C (2004) Proteome analysis of the causative agent of Chagas disease: *Trypanosoma cruzi*. Int J Parasitol **34**:881–886

Parodi-Talice A, Monteiro-Goes V, Arrambide N, Avila AR, Duran R, Correa A, Dallagiovanna B, Cayota A, Krieger M, Goldenberg S, Robello C (2007) Proteomic analysis of metacyclic trypomastigotes undergoing *Trypanosoma cruzi* metacyclogenesis. J Mass Spectrom **42**:1422–1432

Rakauskiene GA, Cenas NK, Kulys JJ (1989) A 'branched' mechanism of the reverse reaction of yeast glutathione reductase. An estimation of the enzyme standard potential values from the steady-state kinetics data. FEBS Lett **243**:33–36

Scott EM, Duncan IW, Ekstrand V (1963) Purification and properties of glutathione reductase of human erythrocytes. J Biol Chem **238**:3928–3933

Serrano A, Rivas J, Losada M (1984) Purification and properties of glutathione reductase from the cyanobacterium *Anabaena* sp. strain 7119. J Bacteriol **158**:317–324

Shigeoka S, Onishi T, Nakano Y, Kitaoka S (1987) Characterization and physiological function of glutathione reductase in *Euglena gracilis* Z. Biochem J **242**:511–515

Szabo M, Lepetit B, Goss R, Wilhelm C, Mustardy L, Garab G (2008) Structurally flexible macro-organization of the pigment-protein complexes of the diatom *Phaeodactylum tricornutum*. Photosynth Res **95**:237–245

Ulusu G, Erat M, Ciftci M, Sakuroulu H, Bakan E (2005) Purification and characterization of glutathione reductase from Sheep Liver. Turk J Vet Anim Sci **29**:1109–1117